DFT based Force Field Development for Noble Gas Adsorption in Metal Organic Frameworks

Supplementary Information

Hakan Demir [a], Jeffery A. Greathouse [b], Chad L. Staiger [c], John J. Perry IV [d] and Mark D. Allendorf [d], David S. Sholl [a]

[a]School of Chemical and Biomolecular Engineering, Georgia Institute of Technology, 311 Ferst Drive NW, Atlanta, Georgia 30332-0100

[b]Geochemistry Department, Sandia National Laboratories, P.O. Box 5800, Albuquerque, New Mexico 87185, USA.
[c]Materials, Devices, and Energy Technologies Department, Sandia National Laboratories, P.O. Box 5800, Albuquerque, New Mexico 87185, USA.

[d]Energy Nanomaterials Department, Sandia National Laboratories, P.O. Box 969, Livermore, California 94551, USA

Table S1. Derived force field parameters for Co-MOF-74

Co-MOF-74	**PBE-D2**		**vdW-DF**		**vdW-DF2**	
	ε(K)	**σ(Å)**	**ε(K)**	**σ(Å)**	**ε(K)**	**σ(Å)**
H-Ar	3.328	3.297	379.310	2.828	52.354	2.832
C-Ar	38.439	3.474	52.363	3.565	53.618	3.470
O-Ar	74.654	3.248	108.820	3.297	164.836	3.120
Co-Ar	154.778	3.109	204.131	3.207	50.980	3.412
H-Xe	111.070	3.045	515.951	2.902	67.529	3.127
C-Xe	50.569	3.746	113.012	3.764	85.467	3.754
O-Xe	126.058	3.435	16.351	4.190	172.063	3.436
Co-Xe	696.420	3.011	708.156	3.024	35.506	3.631

Table S2. Derived force field parameters for Ni-MOF-74

Ni-MOF-74	PBE-D2		vdW-DF		vdW-DF2	
	ε(K)	σ(Å)	ε(K)	σ(Å)	ε(K)	σ(Å)
H-Ar	82.761	2.781	556.072	2.764	96.614	2.706
C-Ar	59.596	3.415	22.316	3.780	62.023	3.439
O-Ar	40.741	3.412	134.217	3.281	134.661	3.154
Ni-Ar	249.157	3.117	239.552	3.135	51.918	3.461
H-Xe	165.573	2.950	465.085	2.950	206.695	2.926
C-Xe	92.418	3.618	136.303	3.742	55.579	3.863
O-Xe	59.839	3.616	6.516	4.487	136.081	3.488
Ni-Xe	426.137	3.169	365.972	3.261	172.595	3.453

Table S3. Derived force field parameters for Zn-MOF-74

Zn-MOF-74	PBE-D2		vdW-DF		vdW-DF2	
	ε(K)	σ(Å)	ε(K)	σ(Å)	ε(K)	σ(Å)
H-Ar	36.141	2.957	106.027	3.021	40.066	2.907
C-Ar	42.925	3.461	107.438	3.441	39.934	3.518
O-Ar	71.147	3.300	133.997	3.229	147.642	3.171
Zn-Ar	420.107	2.901	80.596	3.311	294.334	2.982
H-Xe	67.693	3.113	61.470	3.348	52.803	3.245
C-Xe	93.532	3.576	150.958	3.663	60.448	3.772
O-Xe	51.566	3.697	144.520	3.553	105.028	3.592
Zn-Xe	935.898	2.959	26.229	3.825	667.784	3.090

Table S4. Derived force field parameters for Mg-MOF-74

Mg-MOF-74	PBE-D2		vdW-DF		vdW-DF2	
	ε(K)	σ(Å)	ε(K)	σ(Å)	ε(K)	σ(Å)
H-Ar	37.171	2.943	289.769	2.923	3.345	3.534
C-Ar	41.524	3.487	56.289	3.513	48.664	3.476
O-Ar	62.350	3.330	116.701	3.299	161.272	3.146
Mg-Ar	500.749	2.785	332.103	2.971	217.239	2.982
H-Xe	62.490	3.155	57.441	3.372	47.666	3.301
C-Xe	68.506	3.659	155.331	3.658	57.711	3.796
O-Xe	52.662	3.651	100.188	3.629	114.757	3.564
Mg-Xe	961.205	2.969	82.051	3.565	539.425	3.157

Table S5. Derived force field parameters for ZIF-8

ZIF-8	PBE-D2		vdW-DF		vdW-DF2	
	ε(K)	σ(Å)	ε(K)	σ(Å)	ε(K)	σ(Å)
H-Ar	110.679	2.647	52.469	3.054	176.008	2.616
C-Ar	22.864	3.761	59.430	3.594	29.188	3.723
N-Ar	374.859	2.387	601.377	2.515	166.353	2.411
Zn-Ar	107.188	2.813	107.894	4.756	107.188	2.813
H-Xe	131.705	2.995	31.717	3.367	183.048	2.941
C-Xe	23.440	4.085	44.810	4.116	35.907	4.139
N-Xe	681.114	2.831	1617.740	2.534	1342.592	2.293
Zn-Xe	162.483	3.067	231.913	5.036	162.483	3.067

Table S6. Derived force field parameters for Cu-BTC

Cu-BTC	PBE-D2		vdW-DF		vdW-DF2	
	ε(K)	σ(Å)	ε(K)	σ(Å)	ε(K)	σ(Å)
H-Ar	43.364	2.784	272.412	2.819	101.287	2.623
C-Ar	52.327	3.433	80.119	3.459	76.827	3.390
O-Ar	57.899	3.306	54.718	3.462	68.363	3.282
Cu-Ar	254.085	2.881	332.408	2.911	142.607	2.740
H-Xe	113.358	3.009	65.349	3.336	258.391	2.911
C-Xe	81.649	3.620	134.442	3.729	113.761	3.705
O-Xe	101.198	3.481	73.826	3.729	13.585	4.145
Cu-Xe	600.874	2.948	656.345	3.035	727.904	2.857

Table S7. Comparison of cell parameters of experimental and optimized structures

	CoRE (CSD) MOF/Equivalent CoRE (CSD) MOF/Optimized structure (PBE-D2, vdW-DF, vdW-DF2)					
	a	**b**	**c**	**α**	**β**	**γ**
Co-MOF-74	6.806/15.116/14.737-14.988-15.047	15.116/15.116/14.735-14.979-15.028	15.116/6.806/6.490-6.510-6.540	62.211/81.368/81.567-81.662-81.652	81.368/81.368/81.547-81.666-81.658	98.632/117.789/117.893-117.885-117.846
Mg-MOF-74	6.759/15.194/15.220-15.343-15.345	15.194/15.194/15.211-15.337-15.340	15.194/6.759/6.872-6.988-6.979	62.159/81.473/81.338-81.253-81.270	81.473/81.473/81.336-81.258-81.269	98.527/117.841/117.860-117.708-117.723
Ni-MOF-74	6.770/15.057/14.961-15.198-15.196	15.057/15.057/14.964-15.212-15.199	15.057/6.770/6.189-6.201-6.251	62.205/81.380/82.034-82.194-82.130	81.380/81.380/82.103-82.150-82.083	98.620/117.795/118.105-118.191-118.133
Zn-MOF-74	6.628/15.099/15.196-15.350-15.318	15.099/15.099/15.217-15.370-15.343	15.099/6.628/6.956-7.012-7.047	62.103/81.586/81.259-81.286-81.205	81.586/81.586/81.209-81.170-81.135	98.414/117.897/117.684-117.613-117.581
Cu-BTC	18.627/18.627/18.738-18.914-18.929	18.627/18.627/18.738-18.914-18.929	18.627/18.627/18.738-18.914-18.929	60.000/60.000/60.009-60.003-59.996	60.000/60.000/60.009-60.003-59.996	60.000/60.000/60.009-60.003-59.996
ZIF-8	14.714/14.714/14.657-14.928-14.911	14.714/14.714/14.662-14.940-14.923	14.714/14.714/14.656-14.928-14.910	109.471/109.471/109.456-109.487-109.489	109.471/109.471/109.496-109.393-109.399	109.471/109.471/109.456-109.487-109.489

Table S8. Simulated, experimental surface areas and deviations from experimental surface areas

SA(m^2/g)	PBE-D2	vdW-DF	vdW-DF2	Experimental	Perc. Dev. (%)	Perc. Dev. (%)	Perc. Dev. (%)
Co-MOF-74	1123	1178	1191	1292	13	9	8
Mg-MOF-74	1691	1744	1748	1530	-11	-14	-14
Ni-MOF-74	1118	1151	1161	1199	7	4	3
Zn-MOF-74	1304	1337	1343	973	-34	-37	-38
Cu-BTC	2198	2285	2292	1603	-37	-43	-43
ZIF-8	1314	1430	1422	1391	6	-3	-2

Table S9. Normalized absolute adsorption amount differences with respect to experiments at 1 bar

1bar	PBE-D2	vdW-DF	vdW-DF2	UFF
Ar-Zn-MOF-74	0.551	11.013	2.030	0.312
Xe-Zn-MOF-74	0.791	0.964	0.613	0.222
Ar-Ni-MOF-74	0.116	5.400	0.550	0.246
Xe-Ni-MOF-74	0.082	0.259	0.031	0.154
Ar-Co-MOF-74	0.590	6.690	0.836	0.080
Xe-Co-MOF-74	0.034	0.062	0.088	0.271
Ar-Mg-MOF-74	0.268	9.174	1.917	0.298
Xe-Mg-MOF-74	0.548	0.768	0.453	0.225
Ar-ZIF-8	0.373	6.125	0.448	1.216
Ar-Cu-BTC	0.351	6.261	0.688	0.388
Average	**0.370**	**4.672**	**0.765**	**0.341**
St.dev	0.237	3.734	0.648	0.303

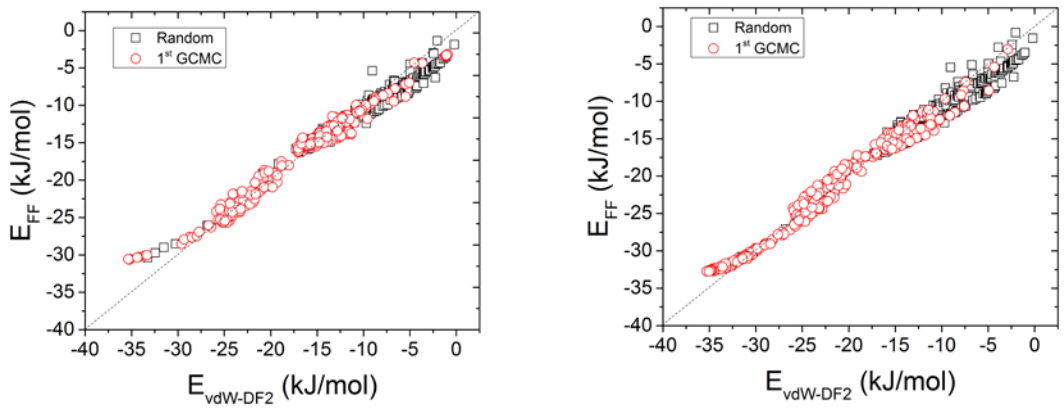

Figure S1. Comparison of vdW-DF2 and fitted FF binding energies for Xe-HKUST-1 (GCMC configurations generated at 100 (left) and 1 bar (right)).

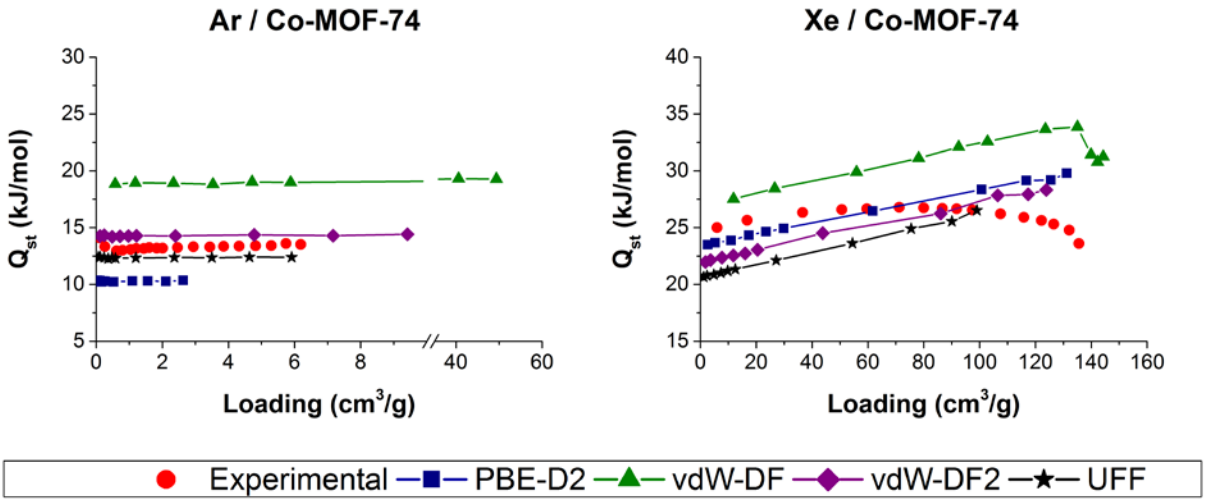

Figure S2. Heat of adsorption values calculated at 292 K for Ar and Xe adsorption in Co-MOF-74

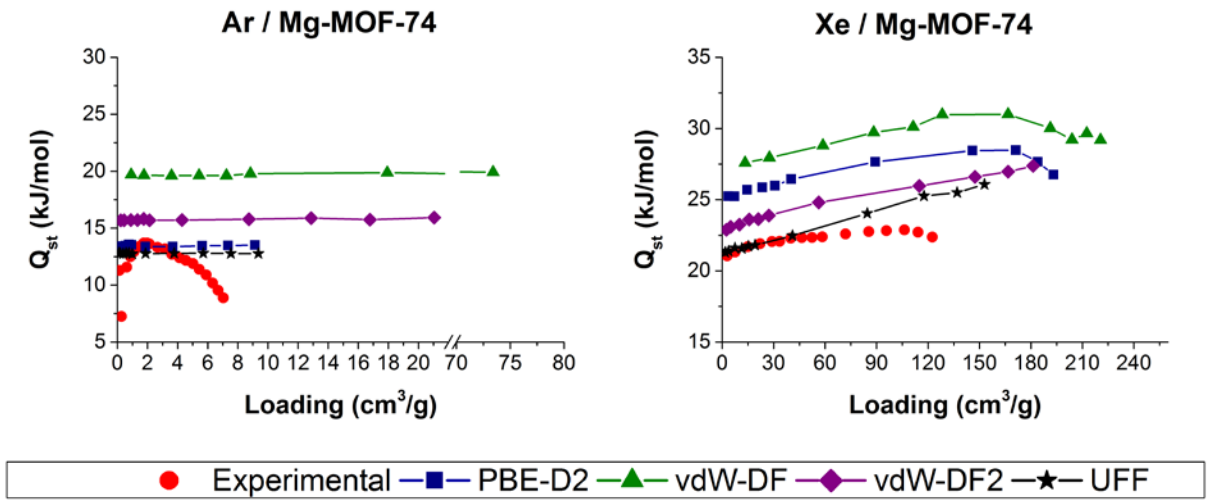

Figure S3. Heat of adsorption values calculated at 292 K for Ar and Xe adsorption in Mg-MOF-74

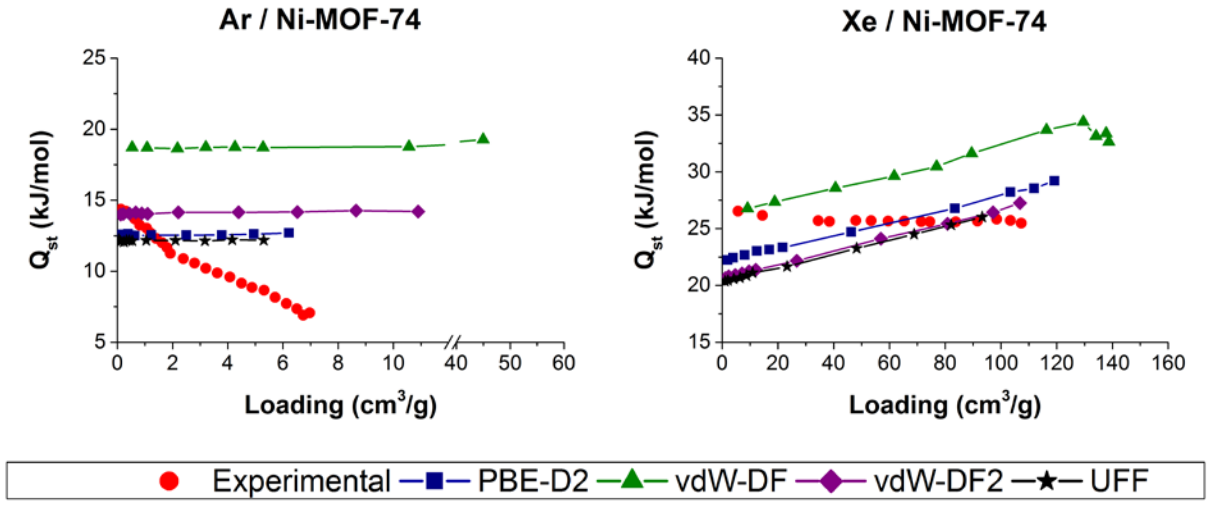

Figure S4. Heat of adsorption values calculated at 292 K for Ar and Xe adsorption in Ni-MOF-74

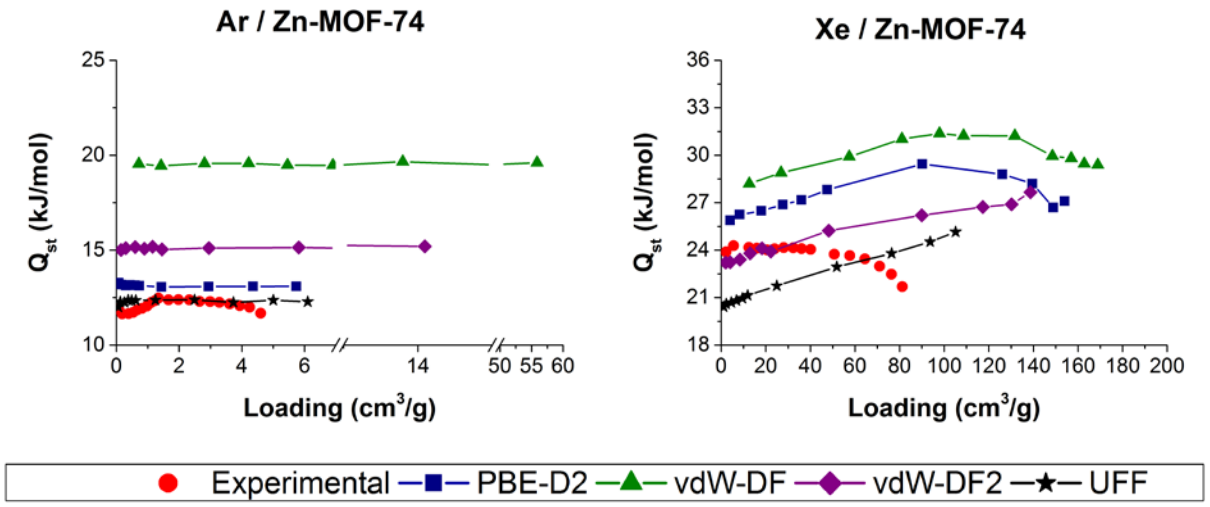

Figure S5. Heat of adsorption values calculated at 292 K for Ar and Xe adsorption in Zn-MOF-74

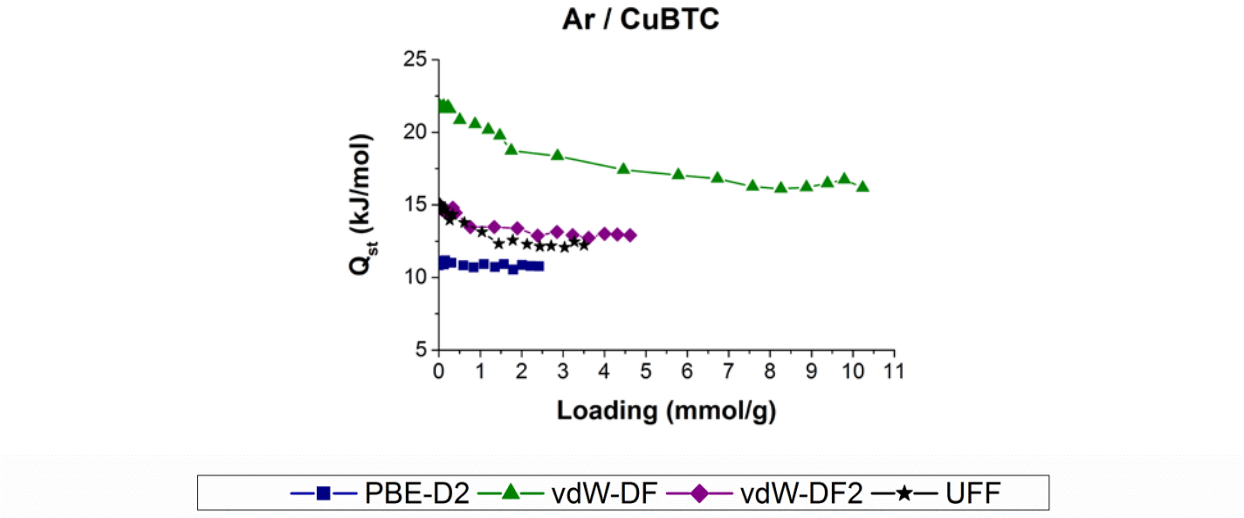

Figure S6. Heat of adsorption values for Ar-Cu-BTC at 308 K

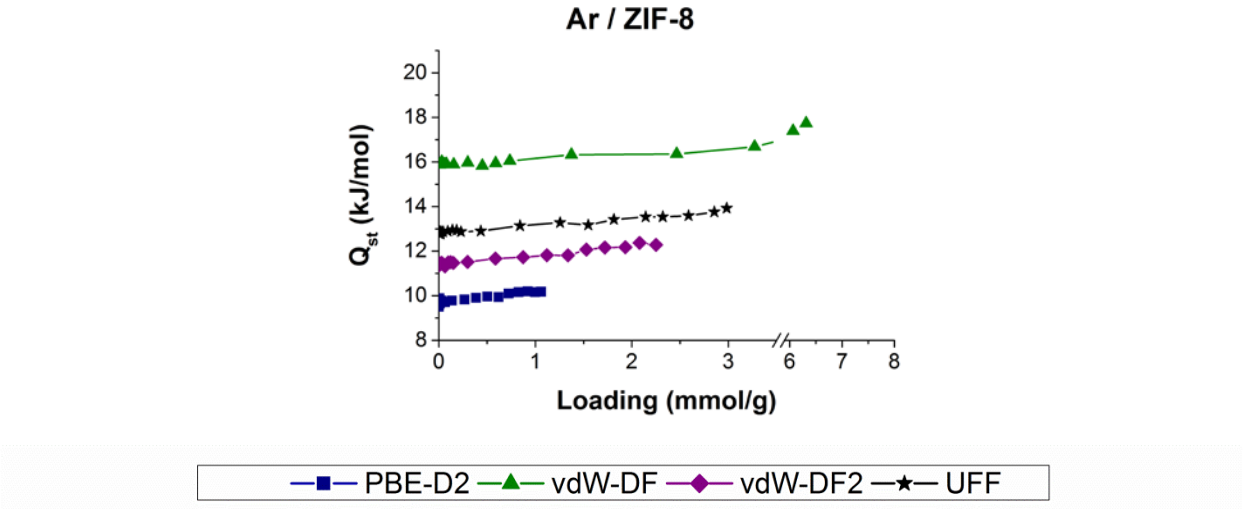

Figure S7. Heat of adsorption values for Ar-ZIF-8 at 308 K

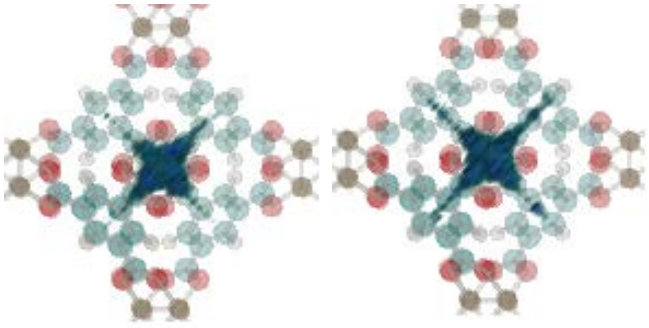

Figure S8. Density plots for Xe adsorption in Cu-BTC using PBE-D2 based FF at 308 K 0.01 bar (left) and 0.1bar (right) (Framework drawn transparent for adsorbate clarity).

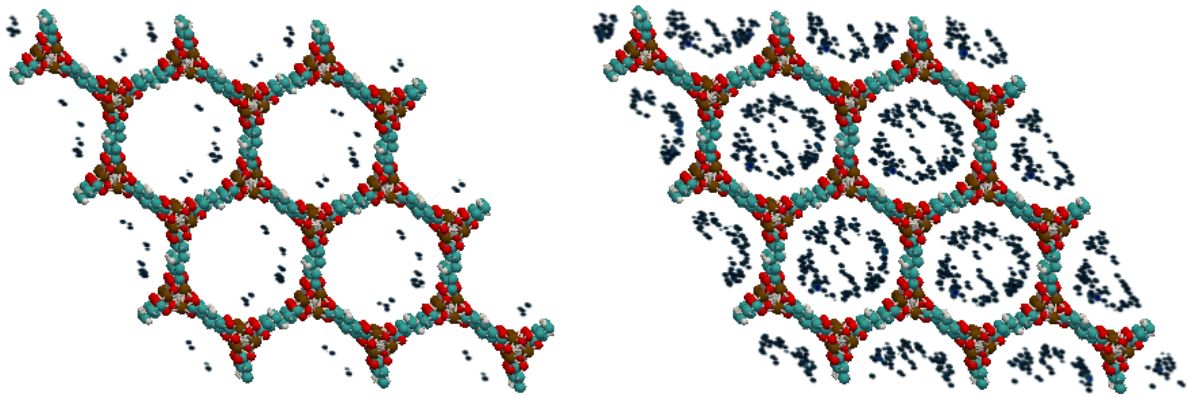

Figure S9. Density plots for Ar adsorption in Co-MOF-74 using PBE-D2 based FF at 292 K and pressures of 10^{-4} bar (left) and 10^{-3} bar (right).

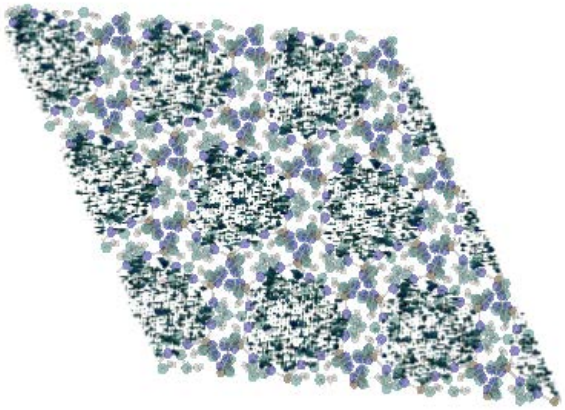

Figure S10. Density plots for Ar adsorption in ZIF-8 using PBE-D2 based FF at 308 K and 0.1 bar (Framework drawn transparent for adsorbate clarity).